


Universal scaling of work statistics in conformal field theory models

Zhaoyu Fei ^{*}

Graduate School of China Academy of Engineering Physics, No. 10 Xibeiwang East Road, Haidian District, Beijing, 100193, China

C. P. Sun[†]Graduate School of China Academy of Engineering Physics, No. 10 Xibeiwang East Road, Haidian District, Beijing, 100193, China
and Beijing Computational Science Research Center, Beijing, 100193, China

(Received 13 January 2021; revised 28 January 2021; accepted 6 April 2021; published 27 April 2021)

We systematically study the work statistics for quantum phase transition. For a quantum system approached by an anisotropic conformal field theory near the critical point, the driving protocol is divided into three different regimes for different quench rates, which reflects the competition between the frozen time and the quench timescale. In each regime, we find universal scaling behaviors in work statistics (after renormalization). It is shown that the critical exponents are determined by the space-time dimension d , the dynamical critical exponent z , the correlation-length exponent ν , and the power-law protocols. These universal scalings in nonequilibrium processes may be found in quantum phase transition by measuring the Loschmidt echo or the Ramsey interferometry.

DOI: [10.1103/PhysRevB.103.144204](https://doi.org/10.1103/PhysRevB.103.144204)

I. INTRODUCTION

In the past decades, quantum quench across the critical point of quantum phase transition attracted much attention both in theories and experiments [1–9], since universal scaling behavior may arise during nonequilibrium processes. Surprisingly, the recent studies have provided a panoramic view of the process: from extremely slow to extremely fast quench (FQ) rates [10–12]. Basically, the driving protocol is divided into three different regimes according to different quench rates. In the slow quench regime, the creation of excitations (topological defects) is usually described by the Kibble-Zurek (KZ) mechanism [13,14] which uncovers the nonadiabatic effect near the critical point. In the fast regime, recent holographic studies [15] also revealed scaling behavior of the renormalized quantities, which is later shown to be universal for quantum field theories flowing from an ultraviolet (UV) fixed point (described by the conformal field theory) [16–18]. In the instantaneous regime, the universal relaxation process to a critical Hamiltonian from a noncritical one was argued [19]. Importantly, it was explicitly shown in Refs. [10,11] that scaling behavior of (renormalized) quantities smoothly interpolates between different regimes with one quench protocol in free scalar and fermion field theories.

The above studies mainly focused on the scaling behavior of the expectation of observables. Nevertheless, due to quantum uncertainty, quantum fluctuations characterized by the cumulants of the excitations [5] and the trajectory work [6,7] also exhibit universal scaling behaviors. In the two-point measurement scheme, the trajectory work is defined as the energy

difference between the initial and final projective measurements [20–23]. As a result, the characteristic function of work [the Fourier transform of the work distribution $P(w)$] $\chi(u)$ reads

$$\chi(u) = \int dw P(w) e^{iuw} = \text{Tr}[e^{iu\hat{H}^H(t_f)} e^{-iu\hat{H}(t_i)} \hat{\rho}], \quad (1)$$

where $\hat{\rho}$ denotes the initial state, $\hat{H}(t_i)$ and $\hat{H}^H(t_f)$ denote Hamiltonians in the Heisenberg picture corresponding to the initial time t_i and final time t_f of the quench. Then, the n th cumulant of work κ_n is defined as the n th-order derivative of $\ln \chi(u)$, $\kappa_n = \partial^n \ln \chi(u) / \partial (iu)^n$. In analog to the partition function encoding essential information about an equilibrium state, the work statistics encodes essential information about the fluctuations in the nonequilibrium process. It allows us to understand the emergence of irreversibility in stochastic thermodynamics (via the fluctuation relations [23–27]). Meanwhile, it is related to other quantities employed to study the nonequilibrium process for quantum many-body systems like the Loschmidt echo [28,29], the Ramsey interferometry [30], and the dynamical quantum phase transition [6,31,32].

However, the close link between the two seemingly irrelevant research fields (stochastic thermodynamics and quantum phase transition) is uncovered through the discovery of the universal scaling of work statistics. The conclusions in Ref. [6] are far from satisfactory because they are based on the quasiparticle picture and only applicable for the slow-quench case. In this paper, we resolve these problems by presenting a panoramic description of the universal scaling behavior of the work cumulants in all three regimes, which implies the competition between the frozen time (KZ mechanism) and the quench timescale. The symmetries of the anisotropic conformal field theory near the critical point make sure of the

^{*}1501110183@pku.edu.cn[†]sunpcp@gscaep.ac.cn

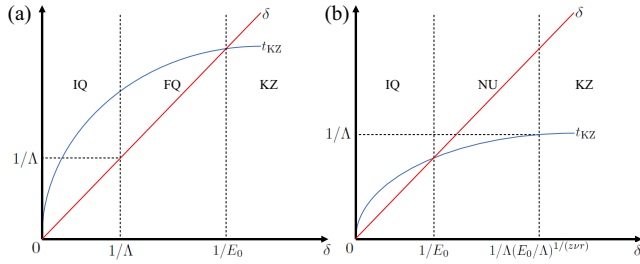


FIG. 1. Two cases for quenches in quantum phase transition. (a) $E_0 \ll \Lambda$. Instantaneous quench (IQ) regime, fast quench (FQ) regime, and Kibble-Zurek (KZ) regime. $t_{\text{KZ}} \propto E_0^{-1} (E_0 \delta)^{1/(z+\nu)}$. (b) $E_0 > \Lambda$. Instantaneous quench (IQ) regime, nonuniversal (NU) regime, and Kibble-Zurek (KZ) regime.

universality of the scaling behaviors. Compared with previous results [6] in the quasiparticle picture, our results are obtained by using the dimensional analysis and are thus universal. Moreover, we give a clear description of the renormalization procedure in nonequilibrium processes. Actually, similar to the *minimal subtraction scheme*, the divergent part of quantities is renormalized by subtracting its value in the adiabatic limit (sudden quench limit) for the UV renormalization [infrared (IR) renormalization]. The higher order corrections (cutoff dependent) may arise in some cases. Finally, our observations are explicitly verified in an exactly solvable model: a scalar field with changing mass.

II. QUANTUM QUENCH IN QUANTUM PHASE TRANSITION

In a (second-order) quantum phase transition, the energy gap E_g , the relaxation time τ , and the correlation length ξ [2,3] scale as

$$E_g \sim |\lambda|^{z\nu}, \tau \sim |\lambda|^{-z\nu}, \xi \sim |\lambda|^{-\nu}, \quad (2)$$

where λ measures the distance from the critical point. If λ is controlled according to a time-dependent protocol which starts from $t = t_i$ and ends at $t = t_f$ and changes over a timescale δ [see Eqs. (3) and (4)], we call this quantum quench when the initial state is the vacuum, regardless of the rate of change [12]. We only consider global quench which keeps the space-translation symmetry in the following. Also, we assume the quench process passes through or approaches a critical point at $t = 0$ and the protocol exhibits the power-law behavior near the critical point:

$$\lambda(t) \sim (t/\delta)^r. \quad (3)$$

Without loss of generality, it follows from Eqs. (2) and (3) that the time-dependent energy-gap protocol $E_g(t)$ reads

$$E_g(t) = E_0 f(t/\delta), \quad (4)$$

where E_0 denotes the energy scale, $f(x) \rightarrow |x|^{z\nu r}$ when $|x| \rightarrow 0$. We also assume $f(x)$ is up to $O(1)$ all the time.

Let Λ denote the UV cutoff scale. Then, according to different quench rates, the protocols can be divided into three different regimes in two cases: $E_0 \ll \Lambda$ or $E_0 > \Lambda$ (Fig. 1). We only discuss the case $E_0 \ll \Lambda$ in the following (for the case $E_0 > \Lambda$, see [33]).

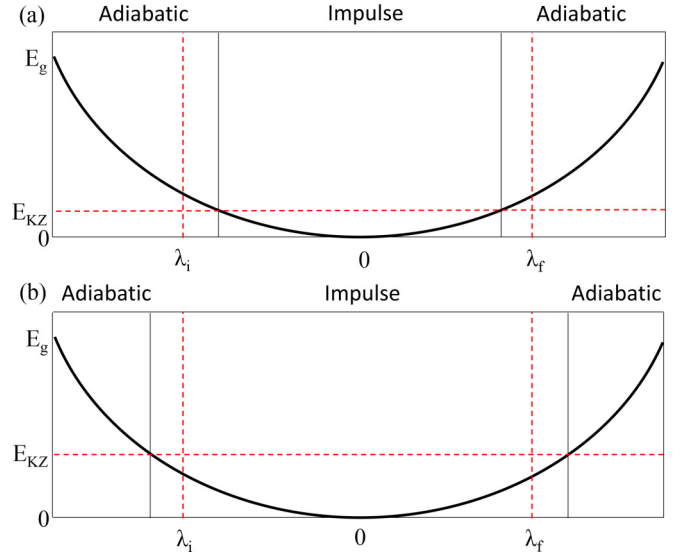


FIG. 2. The competition between the frozen time t_{KZ} and the quench timescale δ in the adiabatic-impulse-adiabatic stages. The black solid line denotes the energy gap E_g . (a) the Kibble-Zurek regime. A part of the protocol is inside the impulse stage ($t_{\text{KZ}} < \delta$). (b) The fast quench regime. The whole protocol is inside the impulse stage ($t_{\text{KZ}} > \delta$).

A. Kibble-Zurek regime

When the quench rate is slow compared to the initial gap ($E_0 \delta \gg 1$), many systems show KZ scaling [3,4,13,14,34,35]. The quench process can be approximated by the adiabatic-impulse-adiabatic stages [see Fig. 2(a)]. Because the quench rate is slow, the quench process is adiabatic unless the adiabatic condition

$$\frac{1}{E_g(t)^2} \frac{dE_g(t)}{dt} \ll 1 \quad (5)$$

is broken near the critical point (i.e., in the impulse stage) due to the zero-energy gap. The boundaries of the impulse stage are at times $t = \pm t_{\text{KZ}}$ (frozen time), which follows from Eqs. (4) and (5), and reads

$$t_{\text{KZ}} \propto E_0^{-1} (E_0 \delta)^{\frac{z\nu r}{1+z\nu r}}. \quad (6)$$

Then, the corresponding correlation length ξ_{KZ} and energy gap E_{KZ} read

$$\xi_{\text{KZ}} \sim |\lambda(t_{\text{KZ}})|^{-\nu} \sim \delta^{\frac{\nu r}{1+z\nu r}}, \quad (7)$$

$$E_{\text{KZ}} = E_g(t_{\text{KZ}}) \sim \delta^{-\frac{z\nu r}{1+z\nu r}}. \quad (8)$$

If the unique length scale in the impulse stage is ξ_{KZ} , the expectation value of a given operator \hat{O}_Δ (which are independent of λ) scales as powers of ξ_{KZ} [12],

$$\langle O_\Delta \rangle_{\text{re}} \sim \xi_{\text{KZ}}^{-\Delta}, \quad (9)$$

where the subscript re denote quantities after renormalization (see the next section) and Δ is the scaling dimension of the operator $\hat{O}_\Delta(t)$. In other words:

$$\langle O_\Delta \rangle_{\text{re}} \sim \delta^{-\frac{\Delta\nu r}{1+z\nu r}}. \quad (10)$$

The energy of the final state $\langle H(t) \rangle_r$ should be proportional to the final energy gap. When the process ends in the adiabatic stage, $E_g(t) \sim E_0$, we have

$$\langle H(t) \rangle_{\text{re}} \propto V_{d-1} E_0 \xi_{\text{KZ}}^{-(d-1)} \sim \delta^{-\frac{(d-1)\nu r}{1+z\nu r}} \quad (11)$$

by using the dimensional analysis, where d is the space-time dimension, V_{d-1} is the volume of the system. Similarly for work statistics [6], the n th-order cumulant work moment κ_n is obtained as

$$(\kappa_n)_{\text{re}} \propto V_{d-1} E_0^n \xi_{\text{KZ}}^{-(d-1)} \sim \delta^{-\frac{(d-1)\nu r}{1+z\nu r}}. \quad (12)$$

When the process ends in the impulse stage, $E_g(t) \sim E_{\text{KZ}}$, we have

$$(\kappa_n)_{\text{re}} \propto V_{d-1} E_{\text{KZ}}^n \xi_{\text{KZ}}^{-(d-1)} \sim \delta^{-\frac{(d-1+z\nu)r}{1+z\nu r}}. \quad (13)$$

It is emphasized that Eqs. (12) and (13) are obtained by using the dimensional analysis regardless of the independent quasi-particle picture in Ref. [6]. Moreover, the KZ scaling is closely related to the conformal field theory where the exponents z , ν , δ imply the scale symmetry of the field.

B. Fast quench

As the quench timescale δ increases, both E_{KZ} and the range of the impulse stage increase. When the whole driving protocol is included in the impulse stage ($t_{\text{KZ}} > \delta$), the timescale for the nonadiabatic effect changes from t_{KZ} to δ and the KZ scaling is invalid [see Fig. 2(b)]. Here, this regime is called the FQ regime, $E_0 \delta \ll 1 \ll \Lambda \delta$, and we show new scaling behavior in the following.

Because the system is always near the critical point in the FQ regime, we evaluate quantities by using perturbation expansion. In particular, consider a generic action near the critical point:

$$S[\hat{\phi}, \hat{O}_\Delta] = S_{\text{CFT}}[\hat{\phi}, \hat{O}_\Delta] - \int dt \int d^{d-1}x \lambda(t) \hat{O}_\Delta(\mathbf{x}, t). \quad (14)$$

Here $\lambda(t) = \lambda_0 h(t/\delta)$ is the protocol which starts from $\lambda_i = \lambda_0 h(t_i/\delta)$ and ends at $\lambda_f = \lambda_0 h(t_f/\delta)$, $\hat{O}_\Delta(\mathbf{x}, t)$ is in the Heisenberg picture, S_{CFT} is the anisotropic conformal field theory action (which has scale, translation, and spatial rotation symmetries) [36] describing the UV fixed point, and \hat{O}_Δ is a relevant operator ($\Delta < d$) with the scaling dimension Δ . We assume $g(x)$ is up to $O(1)$ all the time for simplicity. Then, according to Refs. [16,17], $\langle O_\Delta(t) \rangle$ is calculated by using linear response theory ($\hbar = 1$) as

$$\begin{aligned} \langle O_\Delta(\mathbf{x}, t) \rangle &= \langle O_\Delta(\mathbf{x}) \rangle_{\lambda_i} - i\lambda_0 \int_{t_i}^t dt' \int d^{d-1}x' h(t'/\delta) \\ &\quad \times \langle [\hat{O}_\Delta^1(\mathbf{x}, t), \hat{O}_\Delta^1(\mathbf{x}', t')] \rangle_{\lambda_i} + \dots, \end{aligned} \quad (15)$$

where $\hat{O}_\Delta^1(\mathbf{x}, t) = \exp[i\hat{H}(t_0)(t-t_0)] \hat{O}_\Delta(\mathbf{x}) \exp[-i\hat{H}(t_0)(t-t_0)]$ and the expectation values on the right-hand side are evaluated in the initial ground state λ_i . Due to the symmetries of the action, the two-point function behaves as (for the detailed calculation, see Appendix A)

$$\begin{aligned} &\langle [\hat{O}_\Delta^1(\mathbf{x}, t), \hat{O}_\Delta^1(\mathbf{x}', t')] \rangle_{\lambda_i} \\ &= \frac{1}{|\mathbf{x} - \mathbf{x}'|^{2\Delta}} g\left(\frac{|\mathbf{x} - \mathbf{x}'|^z}{t - t'}, \lambda_i |\mathbf{x} - \mathbf{x}'|^{d-1-\Delta+z}\right). \end{aligned} \quad (16)$$

Since the quench process is inside the impulse stage, the characteristic time should be δ . Then according to Eqs. (2) and (4), the characteristic length and energy read $\xi_Q \sim \delta^{1/z}$, $E_Q \sim \delta^{-1}$. It follows from Eq. (16) that

$$\begin{aligned} &g\left(\frac{|\mathbf{x} - \mathbf{x}'|^z}{t - t'}, \lambda_i |\mathbf{x} - \mathbf{x}'|^{d-1-\Delta+z}\right) \\ &= g\left(\frac{|\mathbf{x} - \mathbf{x}'|^z}{t - t'}, 0\right) + O(\lambda_0 \xi_Q^{d-1-\Delta+z}) \end{aligned} \quad (17)$$

and

$$\langle O_\Delta \rangle_{\text{re}} \sim \lambda_0 \delta \xi_Q^{d-1-2\Delta} \sim \delta^{\frac{d-1-2\Delta+z}{z}}. \quad (18)$$

Thus, the results in Refs. [16,17] are a special case ($z = 1$) of ours. Finally, for work statistics, following the similar procedure, we have (see Appendix B)

$$(\kappa_n)_{\text{re}} \sim \delta^{\frac{d-1-2\Delta+2z-nz}{z}}. \quad (19)$$

We would like to emphasize that this approximation is invalid when $\lambda_0 \delta^{(d-1+z-\Delta)/z} > 1$, which is consistent with the condition $E_0 \delta > 1$ since $E_0 \sim |\lambda_0|^{2\nu}$ and $\nu(d-1+z-\Delta) = 1$ (see Appendix A).

C. Instantaneous quench

The fast quench scaling is applicable when only the low-energy modes are excited, i.e., $\Lambda \gg E_0$. When $\Lambda \ll E_0$, the quench rate is fast compared to all physical scales. The evolution of the system can be approximated by its short-time solution and we call this the instantaneous quench regime (IQ). Then, under some conditions, we have (Appendix C)

$$\langle O_\Delta \rangle - \langle O_\Delta \rangle_{\text{su}} \sim \delta^2, \quad (20)$$

$$\kappa_n - (\kappa_n)_{\text{su}} \sim \delta^2, \quad (21)$$

where the subscript su denotes quantities in the sudden quench limit.

In short, our above analysis shows universal scaling behaviors of work statistics [Eqs. (12), (13), (19), (21)] in three different regimes (KZ, FQ, and IQ regimes). This is illustrated in Fig. 3 by the exact solution of the scalar field with changing mass, which is also studied analytically in the following. In the KZ regime, the frozen time determined the universal scaling behavior and work statistics exhibits different scaling behaviors in the two cases (quantum quench ends in the impulse stage or the adiabatic stage), while \hat{O}_Δ exhibits the same scaling behavior. The reason is that the energy gap is λ dependent while \hat{O}_Δ is not. The change from the KZ regime to the FQ regime is due to the competition between the frozen time and the quench time [see Fig. 1(a)]. In the FQ regime, as a result of the symmetries of the anisotropic conformal field, the universal scaling behavior is determined by the scaling dimension of the physical quantities. The above scaling behaviors are applicable when only the low-energy modes are excited, i.e., $\Lambda \gg E_0$, which is broken in the IQ regime.

TABLE I. The first and second cumulants of work for a free field with changing mass in the KZ and FQ regimes.

	Kibble-Zurek regime			Fast quench regime		
	$d = 5$	$d = 4$	$d = 3$	$d = 5$	$d = 4$	$d = 3$
$D^{-1}(\kappa_1)_{\text{re}}, t_f = 0$	$0.014m^{5/2}/\delta^{5/2}$	$0.017m^2/\delta^2$	$0.030m^{3/2}/\delta^{3/2}$	$0.052m^4/\delta$	$-m^4[0.063 \ln(\Lambda\delta) + 0.025]$	$-0.13m^4\delta$
$D^{-1}(\kappa_2)_{\text{re}}, t_f = 0$	$0.032m^3/\delta^3$	$0.030m^{5/2}/\delta^{5/2}$	$0.039m^2/\delta^2$	$0.064m^4/\delta^2$	$0.10m^4/\delta$	$-m^4[0.13 \ln(\Lambda\delta) + 0.050]$
$D^{-1}(\kappa_1)_{\text{re}}, t_f \rightarrow \infty$	$0.051m^3/\delta^2$	$0.080m^{5/2}/\delta^{3/2}$	$0.16m^2/\delta$	$0.010m^4/\delta$	$0.18m^4$	$0.52m^4\delta$
$D^{-1}(\kappa_2)_{\text{re}}, t_f \rightarrow \infty$	$0.13m^4/\delta^2$	$0.22m^{7/2}/\delta^{3/2}$	$0.48m^3/\delta$	$0.016m^4/\delta^2$	$0.21m^4/\delta$	$0.37m^4$

III. RENORMALIZATION

Due to the divergence (UV or IR) of the field theory, the physical quantities should be renormalized [37]. In this section, we discuss the renormalization of $\langle O_\Delta \rangle$ as an example. For other quantities, the procedure of renormalization is applied straightforwardly. When $E_0 \ll \Lambda$, in the KZ and FQ regimes, $\langle O_\Delta \rangle$ is divided into the sum of four parts:

$$\langle O_\Delta \rangle = \langle O_\Delta \rangle_{\text{ad}} + \langle O_\Delta \rangle_{\text{hi}} + \langle O_\Delta \rangle_{\text{re}} + \langle O_\Delta \rangle_{\text{ig}}, \quad (22)$$

where $\langle O_\Delta \rangle_{\text{ad}}$ denotes the zeroth-order adiabatic contribution, $\langle O_\Delta \rangle_{\text{hi}}$ denotes the higher-order adiabatic contribution which is UV divergent, $\langle \hat{O}_\Delta \rangle_{\text{re}}$ is independent of Λ (called *renormalized quantity*), and $\langle O_\Delta \rangle_{\text{ig}}$ vanishes when $\Lambda \rightarrow \infty$.

Due to the adiabatic perturbation theory [35,38,39], when $\lambda(t) - \lambda(t_i) \sim (t - t_i)^r/\delta^r$ and $\lambda(t) - \lambda(t_f) \sim (t - t_f)^r/\delta^r$, the leading order of $\langle O_\Delta \rangle_{\text{hi}}$ is δ^{-2r} (δ^{-r}) if \hat{O}_Δ commutes with $\hat{H}(t_f)$ (or not). For consistency with the last section, $\langle O_\Delta \rangle_{\text{hi}}$ only appears when its order is lower than the order of $\langle O_\Delta \rangle_{\text{re}}$, i.e., $\Delta r v / (1 + z v r) > r$ ($\Delta r v / (1 + z v r) > 2r$) in the KZ regime and $(2\Delta - d + 1 - z)/z > r$ ($(2\Delta - d + 1 - z)/z > 2r$) in the FQ regime [4,6,35,40]. The independence of

$\langle O_\Delta \rangle_{\text{re}}$ on Λ/E_0 reflects the anisotropic conformal symmetries under translation, spatial rotation, and dilation, which enables us to obtain the universal scaling of renormalized quantities.

The above observation is valid when $d - 1 - 2\Delta + z < 0$. When $d - 1 - 2\Delta + z \geq 0$, in the FQ regime, the systems exhibits IR divergence [11,17,18]. Hence, in contrast to Eq. (22), we choose another type of renormalization,

$$\langle O_\Delta \rangle = \langle O_\Delta \rangle_{\text{su}} + \langle O_\Delta \rangle_{\text{in}} + \langle O_\Delta \rangle_{\text{re}} + \langle O_\Delta \rangle_{\text{ig}}, \quad (23)$$

where $\langle O_\Delta \rangle_{\text{in}} \sim \delta^2$ corresponds to the scaling behavior in the instantaneous regime. Also, for consistency with the results in the last section, $\langle O_\Delta \rangle_{\text{in}} \sim \delta^2$ only appears when its order is lower than the order of $\langle O_\Delta \rangle_{\text{re}}$, i.e., $(d - 1 - 2\Delta + z)/z > 2$ [40].

It is concluded that the divergent part of the quantities is renormalized by subtracting its value in the adiabatic limit (sudden quench limit) for the UV renormalization (IR renormalization).

IV. EXAMPLE

A lot of insight into this problem can in fact be obtained by looking at field theories with time-dependent parameters whose time evolution is exactly solvable, e.g., a free scalar field with changing mass in the momentum space and the Schrödinger picture

$$\hat{H}(t) = \frac{V_{d-1}}{2(2\pi)^{d-1}} \int_{k < \Lambda} d^{d-1}k [\hat{P}_k^2 + \omega_k(t)^2 \hat{Q}_k^2] \quad (24)$$

with the canonical quantization $[\hat{Q}_k, \hat{P}_{k'}] = i\delta^{d-1}(\mathbf{k} - \mathbf{k}')$, where the relativistic dispersion relation reads $\omega_k(t) = \sqrt{k^2 + m(t)^2}$ (speed of light $c = 1$), $k^2 = k_1^2 + k_2^2 + \dots + k_{d-1}^2$, and $m(t)$ denotes the changing mass. Hence, the energy-gap protocol is $E_g(t) = \omega_{k=0} = m(t)$ and the critical point is at $m(t) = 0$.

The characteristic function $\chi(u)$ of this system with the initial ground state is analytically solved and results can be found in Refs. [41–43] (for detailed calculation, see Appendix D). Here, for a specific protocol,

$$m(t)^2 = m^2[1 - \cosh^{-2}(t/\delta)], \quad (25)$$

we obtain an exact solution for arbitrary quench rates ($\lambda(t) = m(t)^2/m^2$, $z = 1$, $v = 1/2$, $r = 2$, $\Delta = d - 2$). And for simplicity, we discuss two cases: (1) $t_i \rightarrow -\infty$, $t_f \rightarrow \infty$ and (2) $t_i \rightarrow -\infty$, $t_f = 0$.

We list the analytical results of the first and second work cumulants (renormalized) in KZ and FQ regimes for $d = 5, 4, 3$ in Table I. Here, $D \equiv V_{d-1}\Omega_{d-2}/(2\pi)^{d-1}$, $\Omega_{d-2} \equiv 2(2\pi)^{(d-1)/2}/\Gamma[(d-1)/2]$ is the solid angle in $d - 1$ spatial

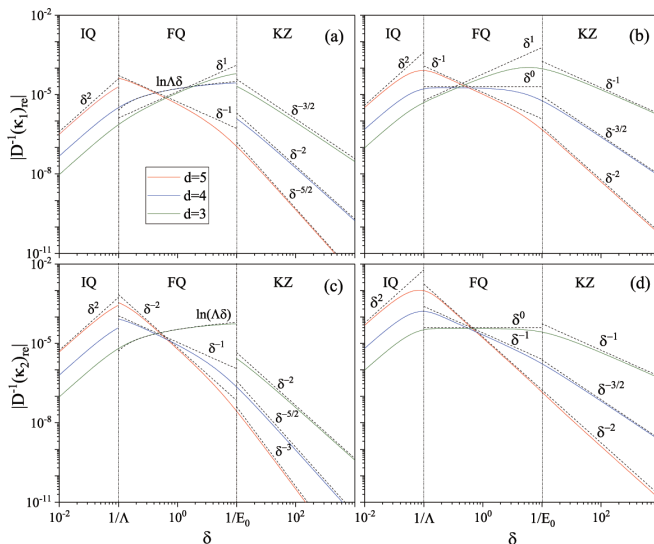


FIG. 3. The first and second cumulants of the work (absolute value) as a function of the quenching rate for a scalar field with time-dependent mass. The parameters are $E_0 = m = 0.1$, $\Lambda = 10$. (a), (c) $t_f = 0$. (b), (d) $t_f \rightarrow \infty$. The solid lines denote $(\kappa_n)_{\text{re}}$ in the Kibble-Zurek regime and fast-quench regime and $(\kappa_n)_{\text{su}} - \kappa_n$ in the instantaneous quench regime. The dashed lines denote the fitting curves.

dimensions, and $\Gamma(s)$ is the gamma function. Moreover, in the IQ regime, the scaling behavior $\kappa_n - (\kappa_n)_{\text{re}} \sim \delta^2$ is also obtained (see Appendix D). In Fig. 3, we show the exact results (solid lines) and the fitting curves (dashed lines) in different cases. These results all verify our predictions in Eqs. (12), (13), (19), and (21).

ACKNOWLEDGMENTS

We thank Y. Chen for helpful discussions. The work was supported by the National Basic Research Program of China (Grant No. 2016YFA0301201), National Natural Science Foundation of China (Grant No. 12088101, No. 11534002), and NSAF (Grant No. U1930403, No. U1930402).

APPENDIX A: ANISOTROPIC CONFORMAL FIELD THEORY

In our paper, the anisotropic conformal field theory means the field action is invariant under anisotropic scale transformation, translation, spatial rotation which form a closed Lie algebra [36]. For the anisotropic scale symmetry, the field action $S_{\text{CFT}}[\phi, O_\Delta]$ is invariant under the following transformation:

$$\mathbf{x} \rightarrow c\mathbf{x}, t \rightarrow c^z t, \phi \rightarrow c^{\Delta_\phi} \phi, O_\Delta \rightarrow c^\Delta O_\Delta, \quad (\text{A1})$$

where z is the dynamical exponent, Δ_ϕ, Δ are the scaling dimensions of the fields ϕ, O_Δ , respectively [36,44]. In addition, for Eq. (14), the total action $S[\phi, O_\Delta]$ is invariant if we also transform λ as

$$\lambda \rightarrow c^{\Delta-d+1-z}\lambda. \quad (\text{A2})$$

If the functional integration measure also has these symmetries, we have the following transformation of the correlation function [44,45]:

$$\begin{aligned} & \langle \hat{O}_\Delta^I(c\mathbf{x}_1, c^z t_1) \hat{O}_\Delta^I(c\mathbf{x}_2, c^z t_2) \cdots \hat{O}_\Delta^I(c\mathbf{x}_n, c^z t_n) \rangle_{c^{\Delta-d+1-z}\lambda} \\ &= c^{-n\Delta} \langle \hat{O}_\Delta^I(\mathbf{x}_1, t_1) \hat{O}_\Delta^I(\mathbf{x}_2, t_2) \cdots \hat{O}_\Delta^I(\mathbf{x}_n, t_n) \rangle_\lambda. \end{aligned} \quad (\text{A3})$$

Since the total action $S[\phi, O_\Delta]$ (for fixed λ) is also invariant under translation and spatial rotation, we have [36,44,45]

$$\begin{aligned} & \langle [\hat{O}_\Delta^I(\mathbf{x}, t), \hat{O}_\Delta^I(\mathbf{x}', t')] \rangle_\lambda \\ &= \frac{1}{|\mathbf{x} - \mathbf{x}'|^{2\Delta}} g\left(\frac{|\mathbf{x} - \mathbf{x}'|^z}{t - t'}, \lambda |\mathbf{x} - \mathbf{x}'|^{d-1-\Delta+tz}\right). \end{aligned} \quad (\text{A4})$$

Thus, both the higher order corrections in Eqs. (15) [16] and (17) are up to the order $O(\lambda_0 \delta^{(d-1-\Delta+tz)/z})$. Moreover, from Eq. (A1), the correlation length behaves as

$$\xi \rightarrow c\xi. \quad (\text{A5})$$

Comparing Eqs. (A2) and (A5) with Eq. (2), we have $c = c^{-\nu(\Delta-d+1-z)}$, i.e., $\nu(d-1+z-\Delta) = 1$ which is also found in Refs. [4,7,46,47].

APPENDIX B: WORK STATISTICS IN THE FAST QUENCH REGIME

In the FQ regime, by using the perturbation theory, from Eq. (14), we have [48]

$$\begin{aligned} \ln \chi(u) &= iu(\lambda_f - \lambda_i) V_{d-1} \langle O_\Delta \rangle_c + iu(\lambda_f^2 - \lambda_i^2) V_{d-1} \\ &\quad \times \int_{-\infty}^{\infty} \frac{d\omega}{2\pi} \frac{G_c^>(\omega)}{\omega} + V_{d-1} \\ &\quad \times \int_{-\infty}^{\infty} \frac{d\omega}{2\pi} \frac{1 - e^{iu\omega}}{\omega^2} A(\omega) G_c^>(\omega) + O(\lambda^3), \end{aligned} \quad (\text{B1})$$

where the subscript c denotes that the quantities are evaluated in the ground state $\lambda = 0$ (critical point) and only connected diagrams are included,

$$A(\omega) = \left| \int_{t_i}^{t_f} dt \dot{\lambda}(t) e^{i\omega t} \right|^2, \quad (\text{B2})$$

and

$$\begin{aligned} G_c^>(\omega) &= \int_{-\infty}^{\infty} ds G_c^>(s) e^{i\omega s}, \quad G_c^>(s) \\ &= (-i)^2 \int d^{d-1}x \langle \hat{O}^I(\mathbf{x}, t) \hat{O}^I(0, 0) \rangle_c. \end{aligned} \quad (\text{B3})$$

Then, from Eq. (B2), it is straightforward to obtain that

$$A(\omega) = A_0(\omega) \equiv \begin{cases} (\lambda_f - \lambda_i)^2 \mathbf{1}_{\{0\}}(\omega) & \text{adiabatic limit} \\ (\lambda_f - \lambda_i)^2 & \text{sudden quench limit,} \end{cases} \quad (\text{B4})$$

where

$$\mathbf{1}_{\{0\}}(\omega) \begin{cases} 1 & \omega = 0 \\ 0 & \omega \neq 0 \end{cases} \quad (\text{B5})$$

is the indicator function. According to Eqs. (22), (23), (B1), and (B4), we have

$$(\ln \chi(u))_{\text{re}} \approx V_{d-1} \int_{-\infty}^{\infty} \frac{d\omega}{2\pi} \frac{1 - e^{iu\omega}}{\omega^2} [A(\omega) - A_0(\omega)] G_c^>(\omega). \quad (\text{B6})$$

Finally, because $G_c^>(\omega) \sim \delta \xi_Q^{d-1-2\Delta}$ [Eqs. (16), (17), and (B3)], $\omega \sim \delta^{-1}$, and $A(\omega) \sim O(1)$ [Eq. (B2)], we have

$$(\ln \chi(u))_{\text{re}} \sim \delta^{\frac{d-1-2\Delta+2z}{z}} \quad (\text{B7})$$

and

$$(\kappa_n)_{\text{re}} \propto V_{d-1} E_Q^{n-1} \lambda_0^2 \delta \xi_Q^{d-1-2\Delta} \sim \delta^{\frac{d-1-2\Delta+2z-nz}{z}}. \quad (\text{B8})$$

For a scalar field with changing mass [Eq. (24)], from Eqs. (25), (B2), and (B3), we have

$$A(\omega) = \left| \int_{-\infty}^{t_f} dt \dot{\lambda}(t) e^{i\omega t} \right|^2 = 16 \left| \sum_{l=1}^{\infty} \frac{l^2}{l + i\omega\delta/2} (-\eta)^l \right|^2, \quad (\text{B9})$$

where $\eta = e^{2t_f/\delta}$ and

$$G_c^>(\omega) = \frac{-Dm^4}{8} \int_0^\Lambda dk k^{d-4} 2\pi \delta(\omega - 2k). \quad (\text{B10})$$

The series converges when $t_f < 0$, but our following results [except Eq. (B14)] are still valid when $t_f > 0$ by using analytic continuation. Then, we obtain

$$\begin{aligned} & (\ln \chi(u))_{\text{re}} \\ &= \frac{Dm^4}{2} \int_0^\Lambda dk k^{d-6} (e^{2iuk} - 1) \\ & \times \begin{cases} \sum_{l,l'} \frac{l^2 l'^2 (l'+k^2 \delta^2)}{(l^2+k^2 \delta^2)(l'^2+k^2 \delta^2)} (-\eta)^{l+l'} & d \geq 5 \\ \sum_{l,l'} \left[\frac{l^2 l'^2 (l'+k^2 \delta^2)}{(l^2+k^2 \delta^2)(l'^2+k^2 \delta^2)} - ll' \right] (-\eta)^{l+l'} & d < 5. \end{cases} \end{aligned} \quad (\text{B11})$$

Let $\Lambda/m \rightarrow \infty$, from Eq. (B11), we have

$$(\kappa_1)_{\text{re}} = Dm^4 \times \begin{cases} \frac{\pi \eta^2 (\eta^3 + 5\eta^2 - 5\eta + 15)}{30(\eta+1)^5} \delta^{-1} & d = 5 \\ \frac{-\eta^2}{(\eta+1)^4} \ln(\Lambda \delta) + C_1 & d = 4 \\ \frac{\pi \eta^2 (\eta-3)}{6(\eta+1)^3} \delta & d = 3 \end{cases} \quad (\text{B12})$$

and

$$(\kappa_2)_{\text{re}} = 2Dm^4 \times \begin{cases} \left[\frac{\eta^2 (\eta-1)^2}{(\eta+1)^6} \ln(\Lambda \delta) + C_2 \right] \delta^{-2} & d = 5 \\ \frac{\pi \eta^2 (\eta^3 + 5\eta^2 - 5\eta + 15)}{30(\eta+1)^5} \delta^{-1} & d = 4 \\ \frac{-\eta^2}{(\eta+1)^4} \ln(\Lambda \delta) + C_1 & d = 3, \end{cases} \quad (\text{B13})$$

where

$$\begin{aligned} C_1 &= \sum_{l,l'} \frac{ll' (l \ln l' + l' \ln l)}{l+l'} (-\eta)^{l+l'}, \\ C_2 &= - \sum_{l,l'} \frac{l^2 l'^2 (l \ln l + l' \ln l')}{l+l'} (-\eta)^{l+l'}. \end{aligned} \quad (\text{B14})$$

When $t_f = 0$, numerical calculation of Eq. (B14) shows $C_1 = -0.025$ and $C_2 = 0.032$. When $t_f \rightarrow \infty$, from Eq. (B13), we have

$$(\kappa_2)_{\text{re}} = 2Dm^4 \times \begin{cases} C_2 \delta^{-2} & d = 5 \\ \frac{\pi}{30} \delta^{-1} & d = 4 \\ C_1 & d = 3. \end{cases} \quad (\text{B15})$$

Here, because

$$A(\omega) = \frac{\pi^2 \omega^4 \delta^4}{\sinh^2(\pi \omega \delta / 2)}, \quad (\text{B16})$$

in this case [Eq. (B2)], the calculation of $(\kappa_2)_{\text{re}}$ shows $C_1 = 3\zeta(3)/(2\pi^2)$ and $C_2 = 15\zeta(5)/(2\pi^4)$.

APPENDIX C: SHORT-TIME EVOLUTION

In the IQ regime, the evolution of the system can be approximated by its short-time solution. When $\delta \rightarrow 0$, $t_1 = s_1 \delta$, $t_0 = 0$, the time evolution operator $\hat{U}(t_1, t_0) = \mathcal{T} e^{-i \int_0^{t_1} dt [\hat{H}_0 + \lambda(t) \hat{H}_1]}$ is approximated as

$$\begin{aligned} \hat{U}(t_1, t_0) &= 1 - i\delta \int_0^{s_1} ds [\hat{H}_0 + \lambda(s\delta) \hat{H}_1] \\ & - \delta^2 \int_0^{s_1} ds \int_0^s ds' [\hat{H}_0 + \lambda(s\delta) \hat{H}_1] \\ & \times [\hat{H}_0 + \lambda(s'\delta) \hat{H}_1] + O(\delta^3), \end{aligned} \quad (\text{C1})$$

where \mathcal{T} denotes the time-ordered operator. For further discussion, let $|E_n(t)\rangle$ denote the instantaneous eigenstate of the time-dependent Hamiltonian, $[\hat{H}_0 + \lambda(t) \hat{H}_1] |E_n(t)\rangle = E_n(t) |E_n(t)\rangle$, $|E_0(t)\rangle$ denote the ground state. Then, we have

$$\langle E_n(t_1) | \hat{H}_1 | E_0(t_0) \rangle = \frac{E_n(t_1) - E_0(t_0)}{\lambda_f - \lambda_i} \langle E_n(t_1) | E_0(t_0) \rangle. \quad (\text{C2})$$

Thus, let $\alpha_n = \langle E_n(t_1) | \hat{U}(t_1, t_0) | E_0(t_0) \rangle$ and $\alpha_n^0 = \langle E_n(t_1) | E_0(t_0) \rangle$ denote the transition probability amplitude for the IQ and sudden quench; it follows from Eqs. (C1) and (C2) that

$$\begin{aligned} \alpha_n &= \alpha_n^0 \left\{ 1 - i\delta s_1 E_0(t_0) - i\delta \frac{E_n(t_1) - E_0(t_0)}{\lambda_f - \lambda_i} \right. \\ & \times \int_0^{s_1} ds [\lambda(s\delta) - \lambda_i] \left. \right\} \\ & - \delta^2 \int_0^{s_1} ds \int_0^s ds' \langle E_n(t_1) | [\hat{H}_0 + \lambda(s\delta) \hat{H}_1] \\ & \times [\hat{H}_0 + \lambda(s'\delta) \hat{H}_1] | E_0(t_0) \rangle + O(\delta^3). \end{aligned} \quad (\text{C3})$$

Thus, it is easy to check that if an operator \hat{A} satisfies $\langle E_m(t_1) | \hat{A} | E_n(t_1) \rangle (\alpha_m^0)^* \alpha_n^0 = \langle E_n(t_1) | \hat{A} | E_m(t_1) \rangle (\alpha_n^0)^* \alpha_m^0$ (* denotes the complex conjugate), we have

$$\langle A \rangle - \langle A \rangle_{\text{su}} \sim \delta^2, \quad (\text{C4})$$

where $\langle A \rangle_{\text{su}} = \langle E_0(t_0) | \hat{A} | E_0(t_0) \rangle$.

APPENDIX D: THE CHARACTERISTIC FUNCTION OF WORK FOR A FREE SCALAR FIELD WITH CHANGING MASS

Because the Hamiltonian of the field [Eq. (24)] is a quadratic form of \hat{P}_k and \hat{Q}_k , we obtain the cumulant characteristic function of work $\ln \chi(u)$ by using the representation of the Lie group [43] as

$$\begin{aligned} \ln \chi(u) &= \frac{D}{2} \int_0^\Lambda dk k^{d-2} \{ iu [\omega_k(t_f) - \omega_k(t_i)] \\ & - \ln[1 + n_k - n_k e^{2iu\omega_k(t_f)}] \}, \end{aligned} \quad (\text{D1})$$

where $D \equiv V_{d-1} \Omega_{d-2} / (2\pi)^{d-1}$, $\Omega_{d-2} \equiv 2(2\pi)^{(d-1)/2} / \Gamma[(d-1)/2]$ is the solid angle in $d-1$ spatial dimensions, $\Gamma(s)$ is the Gamma function,

$$n_k = \frac{\omega_k(t_f)}{4\omega_k(t_i)} \left[y_k(t_f)^2 + \bar{y}_k(t_f)^2 + \frac{\dot{y}_k(t_f)^2 + \dot{\bar{y}}_k(t_f)^2}{\omega_k(t_f)^2} \right] - \frac{1}{2}, \quad (\text{D2})$$

the overhead dot denotes the time derivative, and $y_k(t)$, $\bar{y}_k(t)$ are the general solutions of the following equation:

$$\ddot{y}(t) + \omega_k(t) y(t) = 0, \quad (\text{D3})$$

with the initial condition $\{y_k(t_i), \dot{y}_k(t_i), \bar{y}_k(t_i), \dot{\bar{y}}_k(t_i)\} = \{1, 0, 0, \omega_k(t_i)\}$. Then, we have

$$\begin{aligned} \kappa_1 &= \mu + D \int_0^\Lambda dk k^{d-2} \omega_k(t_f) n_k, \\ \kappa_2 &= D \int_0^\Lambda dk k^{d-2} 2\omega_k(t_f)^2 n_k (1 + n_k), \end{aligned} \quad (\text{D4})$$

where

$$\mu = \frac{D}{2} \int_0^\Lambda dk k^{d-2} [\omega_k(t_f) - \omega_k(t_i)]. \quad (\text{D5})$$

It follows from Eq. (D4) that n_k denotes the average number of the excited bosons in mode k after quench and μ denotes the work done without any excitation (i.e., zeroth-order adiabatic contribution).

For the specific protocol [Eq. (25) with $t_i \rightarrow -\infty$], we obtain the following results:

(1) KZ regime ($m\delta \gg 1$). In this regime, the characteristic momentum is $k_c \sim \sqrt{m/\delta} \ll m$ [10]. Hence, from the exact solution of Eq. (D3) (Appendix E), when $t_f = 0$, we have

$$n_k \approx \frac{\sqrt{m\delta} e^{-3\pi q_k^2/4} (e^{\pi q_k^2} + 1)}{4\pi q_k \sqrt{q_k^2 + m\delta}} \left[\left| \Gamma\left(\frac{3}{4} + \frac{iq_k^2}{4}\right) \right|^2 + \frac{q_k^2}{4} \left| \Gamma\left(\frac{1}{4} + \frac{iq_k^2}{4}\right) \right|^2 \right], \quad (\text{D6})$$

where $q_k = k\sqrt{\delta/m}$. From Eqs. (D6) and letting $\Lambda\sqrt{\delta/m} \rightarrow \infty$ (only low-energy modes can be excited), we have

$$(\kappa_1)_{\text{re}} = D \left(\frac{m}{\delta}\right)^{d/2} \times \begin{cases} 0.014 & d = 5 \\ 0.017 & d = 4 \\ 0.030 & d = 3 \end{cases} \quad (\text{D7})$$

and

$$(\kappa_2)_{\text{re}} = D \left(\frac{m}{\delta}\right)^{(d+1)/2} \times \begin{cases} 0.032 & d = 5 \\ 0.030 & d = 4 \\ 0.039 & d = 3. \end{cases} \quad (\text{D8})$$

Moreover, due to the power-law decay of Eq. (D6) ($n_k \rightarrow 1/(64q_k^8)$ when $q_k \rightarrow \infty$), we cannot let $\Lambda\sqrt{\delta/m} \rightarrow \infty$ when $(d-1+n)/2 \geq 4$, which results in that $(\kappa_n)_{\text{hi}} \sim \delta^{-4} \ln(\Lambda\delta)$ when $(d-1+n)/2 = 4$ and $(\kappa_n)_{\text{hi}} \sim \delta^{-4}$ when $(d-1+n)/2 > 4$.

Similarly, when $t_f \rightarrow \infty$, according to Appendix E and Eq. (D1), we have

$$n_k \approx e^{-\pi q_k^2}, \quad (\text{D9})$$

and

$$\ln \chi(u) = iu\mu + \frac{D\Gamma[(d-1)/2]}{4\pi^{(d-1)/2}} \times \left(\frac{m}{\delta}\right)^{(d-1)/2} \text{Li}_{(d+1)/2}(e^{2i\mu} - 1), \quad (\text{D10})$$

where $\text{Li}_n(s) = \sum_{l=1}^{\infty} s^l/l^n$ is the polylogarithm function. Hence, we have $(\kappa_n)_{\text{re}} \sim (m/\delta)^{(d-1)/2}$ for any n . Moreover, due to the exponential decay of n_k when $k \rightarrow \infty$, we can let $\Lambda\sqrt{\delta/m} \rightarrow \infty$ all the time, i.e., $(\kappa_n)_{\text{hi}} = 0$, which is consistent with the fact that $d^n \lambda(t)/dt^n = 0$ for any n when $t \rightarrow \pm\infty$.

(2) Fast quench regime ($m\delta \ll 1 \ll \Lambda\delta$). Here, the characteristic momentum is $k_c \sim m \ll \sqrt{m/\delta}$ [10]. For convenience of calculation, we use perturbation theory to calculate $\ln \chi(u)$ (see Appendix B). Then we have,

when $t_f = 0$,

$$(\kappa_1)_{\text{re}} = Dm^4 \times \begin{cases} \frac{\pi}{60} \delta^{-1} & d = 5 \\ -\frac{1}{16} \ln(\Lambda\delta) - 0.025 & d = 4 \\ -\frac{\pi}{24} \delta & d = 3 \end{cases} \quad (\text{D11})$$

and

$$(\kappa_2)_{\text{re}} = 2Dm^4 \times \begin{cases} 0.032\delta^{-2} & d = 5 \\ \frac{\pi}{60} \delta^{-1} & d = 4 \\ -\frac{1}{16} \ln(\Lambda\delta) - 0.025 & d = 3 \end{cases} \quad (\text{D12})$$

when $t_f \rightarrow \infty$,

$$(\kappa_1)_{\text{re}} = Dm^4 \times \begin{cases} \frac{\pi}{30} \delta^{-1} & d = 5 \\ \frac{3\zeta(3)}{2\pi^2} & d = 4 \\ \frac{\pi}{6} \delta & d = 3 \end{cases} \quad (\text{D13})$$

and

$$(\kappa_2)_{\text{re}} = 2Dm^4 \times \begin{cases} \frac{15\zeta(5)}{2\pi^4} \delta^{-2} & d = 5 \\ \frac{\pi}{30} \delta^{-1} & d = 4 \\ \frac{3\zeta(3)}{2\pi^2} & d = 3, \end{cases} \quad (\text{D14})$$

where $\zeta(s)$ is the Riemann zeta function. Also, $(\kappa_n)_{\text{hi}} \sim \delta^{-4} \ln(\Lambda\delta)$ appears when $d-3-n=4$ and $(\kappa_n)_{\text{hi}} \sim \delta^{-4}$ appears when $d-3-n > 4$. This is due to the fact that when $t_f = 0$ and $\omega \rightarrow \infty$, $A(\omega) \rightarrow \omega^{-4}$ [Eq. (B9)].

(3) Instantaneous quench regime ($\Lambda\delta \ll 1$). In this regime, according to Appendix E, we have, when $t_f \rightarrow \infty$,

$$n_k \approx \frac{m^4 \delta^2}{k^2 + m^2}; \quad (\text{D15})$$

when $t_f = 0$,

$$n_k \approx \frac{(k - \sqrt{k^2 + m^2})^2 + (1 - 2 \ln 2)m^4 \delta^2}{4k\sqrt{k^2 + m^2}}. \quad (\text{D16})$$

Hence, from Eqs. (D15) and (D16), we have $\ln \chi(u) - (\ln \chi(u))_{\text{su}} \sim \delta^2$ and $\kappa_n - (\kappa_n)_{\text{su}} \sim \delta^2$.

APPENDIX E: EXACT SOLUTIONS OF EQ. (D3)

According to Ref. [10,17], the general solutions of Eq. (D3) [with the protocol Eq. (25)], $u_k(t)$ and $u_k^*(t)$, read (when $t_i \rightarrow -\infty$)

$$u_k(t) = \frac{2^{i\omega_k(t_i)\delta} [\cosh(t/\delta)]^{2\alpha}}{B_1 B_2 - B_1' B_2'} \left[B_2 {}_2F_1\left(a, b; \frac{1}{2}; -\sinh^2(t/\delta)\right) + B_1 \sinh(t/\delta) {}_2F_1\left(a + \frac{1}{2}, b + \frac{1}{2}; \frac{3}{2}; -\sinh^2(t/\delta)\right) \right], \quad (\text{E1})$$

with the initial conditions when $t \rightarrow -\infty$, $\{u_k(t), u_k^*(t)\} \rightarrow \{e^{-i\omega_k(t_i)t}, e^{i\omega_k(t_i)t}\}$, where

$$B_1 = \frac{\Gamma(1/2)\Gamma(b-a)}{\Gamma(b)\Gamma(1/2-a)}, \quad B_1' = \frac{\Gamma(1/2)\Gamma(a-b)}{\Gamma(a)\Gamma(1/2-b)},$$

$$B_2 = \frac{\Gamma(3/2)\Gamma(b-a)}{\Gamma(b+1/2)\Gamma(1-a)}, \quad B_2' = \frac{\Gamma(3/2)\Gamma(a-b)}{\Gamma(a+1/2)\Gamma(1-b)},$$

$$a = \alpha + i\omega_k(t_i)\delta/2, \quad b = \alpha - i\omega_k(t_i)\delta/2,$$

$$\alpha = \frac{1 - \sqrt{1 - 4m^2\delta}}{4}, \quad (\text{E2})$$

and

$${}_2F_1(a, b, c; s) = \sum_{n=0}^{\infty} \frac{(a)_n (b)_n s^n}{(c)_n n!} \quad (\text{E3})$$

denotes the usual hypergeometric function, and $(x)_n = x(x+1)\cdots(x+n-1)$ ($(x)_0 = 1$). Thus, when $t \rightarrow 0$, we have

$$u_k(t) \rightarrow \frac{2^{i\omega_k(t_i)\delta}}{B'_1 B_2 - B_1 B'_2} \left(B_2 + \frac{B_1}{\delta} \right). \quad (\text{E4})$$

And when $t \rightarrow \infty$, we have

$$u_k(t) \rightarrow \frac{2^{i\omega_k(t_i)\delta+1} B_1 B_2}{B'_1 B_2 - B_1 B'_2} e^{-i\omega_k(t_i)\delta} + \frac{B'_1 B_2 + B_1 B'_2}{B'_1 B_2 - B_1 B'_2} e^{-i\omega_k(t_i)\delta}. \quad (\text{E5})$$

Moreover from Eq. (D2), we have

$$n_k = \frac{\omega_k(t_f)}{4\omega_k(t_i)} \left[|u_k(t_f)|^2 + \frac{|\dot{u}_k(t_f)|^2}{\omega_k(t_f)^2} \right] - \frac{1}{2}. \quad (\text{E6})$$

-
- [1] W. H. Zurek, U. Dorner, and P. Zoller, *Phys. Rev. Lett.* **95**, 105701 (2005).
- [2] S. Sachdev, *Quantum Phase Transitions*, 2nd ed. (Cambridge University Press, Cambridge, UK, 2011).
- [3] J. Dziarmaga, *Adv. Phys.* **59**, 1063 (2010).
- [4] A. Polkovnikov, K. Sengupta, A. Silva, and M. Vengalattore, *Rev. Mod. Phys.* **83**, 863 (2011).
- [5] A. del Campo, *Phys. Rev. Lett.* **121**, 200601 (2018).
- [6] Z. Y. Fei, N. Freitas, V. Cavina, H. T. Quan, and M. Esposito, *Phys. Rev. Lett.* **124**, 170603 (2020).
- [7] K. Hódsági and M. Kormos, *SciPost Phys.* **9**, 055 (2020).
- [8] M. Greiner, O. Mandel, T. Esslinger, T. W. Hänsch, and I. Bloch, *Nature* **415**, 39 (2002).
- [9] K. Baumann, R. Mottl, F. Brennecke, and T. Esslinger, *Phys. Rev. Lett.* **107**, 140402 (2011).
- [10] S. R. Das, D. A. Galante, and R. C. Myers, *J. High Energy Phys.* **05** (2016) 164.
- [11] D. Das, S. R. Das, D. A. Galante, R. C. Myers, and K. Sengupta, *J. High Energy Phys.* **11** (2017) 157.
- [12] S. R. Das, *Prog. Theor. Exp. Phys.* **2016**, 12C107 (2016).
- [13] T. W. B. Kibble, *J. Phys. A* **9**, 1387 (1976); *Phys. Rep.* **67**, 183 (1980).
- [14] W. H. Zurek, *Nature (London)* **317**, 505 (1985); *Phys. Rep.* **276**, 177 (1996).
- [15] A. Buchel, L. Lehner, and R. C. Myers, *J. High Energy Phys.* **08** (2012) 049; A. Buchel, L. Lehner, R. C. Myers, and A. van Niekerk, *ibid.* **05** (2013) 067; A. Buchel, R. C. Myers, and A. van Niekerk, *Phys. Rev. Lett.* **111**, 201602 (2013).
- [16] S. R. Das, D. A. Galante, and R. C. Myers, *Phys. Rev. Lett.* **112**, 171601 (2014).
- [17] S. R. Das, D. A. Galante, and R. C. Myers, *J. High Energy Phys.* **02** (2015) 167.
- [18] S. R. Das, D. A. Galante, and R. C. Myers, *J. High Energy Phys.* **08** (2015) 073.
- [19] P. Calabrese and J. Cardy, *Phys. Rev. Lett.* **96** (2006) 136801; *J. Stat. Mech.* (2007) P06008.
- [20] J. Kurchan, *arXiv:cond-mat/0007360*.
- [21] H. Tasaki, *arXiv:cond-mat/0009244*.
- [22] P. Talkner, E. Lutz, and P. Hänggi, *Phys. Rev. E* **75**, 050102(R) (2007).
- [23] M. Esposito, U. Harbola, and S. Mukamel, *Rev. Mod. Phys.* **81**, 1665 (2009).
- [24] K. Sekimoto, *Stochastic Energetics* (Springer-Verlag, Berlin, Heidelberg, 2010).
- [25] C. Jarzynski, *Annu. Rev. Condens. Matter Phys.* **2**, 329 (2011).
- [26] U. Seifert, *Rep. Prog. Phys.* **75**, 126001 (2012).
- [27] R. Dorner, J. Goold, C. Cormick, M. Paternostro, and V. Vedral, *Phys. Rev. Lett.* **109**, 160601 (2012).
- [28] A. Silva, *Phys. Rev. Lett.* **101**, 120603 (2008).
- [29] H. T. Quan, Z. Song, X. F. Liu, P. Zanardi, and C. P. Sun, *Phys. Rev. Lett.* **96**, 140604 (2006).
- [30] R. Dorner, S. R. Clark, L. Heaney, R. Fazio, J. Goold, and V. Vedral, *Phys. Rev. Lett.* **110**, 230601 (2013).
- [31] M. Heyl, A. Polkovnikov, and S. Kehrein, *Phys. Rev. Lett.* **110**, 135704 (2013).
- [32] N. O. Abeling and S. Kehrein, *Phys. Rev. B* **93**, 104302 (2016).
- [33] When $E_0 > \Lambda$, the fast quench regime is replaced by the nonuniversal regime (NU) [Fig. 1(b)], where $E_{KZ} > \Lambda$, $E_0 \delta > 1$ and we do not find universal scaling behavior here.
- [34] A. Polkovnikov, *Phys. Rev. B* **72**, 161201(R) (2005).
- [35] C. De Grandi and A. Polkovnikov, *Quantum Quenching, Annealing and Computation* (Springer, Berlin, 2010), pp. 75–114.
- [36] M. Taylor, *arXiv:0812.0530*.
- [37] In condensed matter physics, the cutoff energy Λ is finite, and the divergence does not exist. However, it is still necessary to do renormalization in this case, because the existence of finite Λ breaks the symmetries of the field and only the Λ -independent (renormalized) quantities exhibit universal scaling behavior.
- [38] C. P. Sun, *J. Phys. A: Math. Gen.* **21**, 1595 (1988).
- [39] G. Rigolin, G. Ortiz, and V. H. Ponce, *Phys. Rev. A* **78**, 052508 (2008).
- [40] When the order of $\langle O \rangle_{\text{hi}}$ or $\langle O \rangle_{\text{in}}$ is equal to the order of $\langle O \rangle_{\text{re}}$, there is an additional logarithm enhancement in the scaling behavior [12,16,35,46].
- [41] S. Deffner and E. Lutz, *Phys. Rev. E* **77**, 021128 (2008).
- [42] P. Smacchia and A. Silva, *Phys. Rev. E* **88**, 042109 (2013).
- [43] Z. Y. Fei and H. T. Quan, *Phys. Rev. Research* **1**, 033175 (2019)
- [44] Y. Nishida and D. T. Son, *Phys. Rev. D* **76**, 086004 (2007).
- [45] P. Francesco, P. Mathieu, and D. Sénéchal, *Conformal Field Theory* (Springer-Verlag, New York, 2012).
- [46] L. Campos Venuti and P. Zanardi, *Phys. Rev. Lett.* **99**, 095701 (2007).
- [47] S. J. Gu, *Int. J. Mod. Phys. B* **24**, 4371 (2010).
- [48] Z. Y. Fei and H. T. Quan, *Phys. Rev. Lett.* **124**, 240603 (2020).